Atmos. Meas. Tech. Discuss., doi:10.5194/amt-2016-9, 2016
Manuscript under review for journal Atmos. Meas. Tech.
Published: 29 January 2016

Atmospheric Measurement Techniques Discussions
Open Access

A review of sources of systematic errors and uncertainties in observations and simulations at 183GHz

Hélène Brogniez[1]*, Stephen English[2], Jean-François Mahfouf[3], *Andreas Behrendt[4], Wesley Berg[5], Sid Boukabara[6], Stefan Alexander Buehler[7], Philippe Chambon[3], Antonia Gambacorta[8], Alan Geer[2], William Ingram[9], E. Robert Kursinski[10], Marco Matricardi[2], Tatyana Odintsova[11], Vivienne Payne[12], Peter Thorne[13], Mikhail Tretyakov[11], Junhong Wang[14]*

[1] LATMOS (IPSL/UVSQ/UPMC/CNRS), 78280, Guyancourt, France

[2] ECMWF, Reading, RG2 9AX, United Kingdom

[3] CNRM/GAME, Météo-France/CNRS, Toulouse, 31057, France

[4] University of Hohenheim, Institute of Physics and Meteorology, D-70599 Stuttgart, Germany

[5] Colorado State University, Fort Collins, USA

[6] NOAA, USA

[7] Meteorological Institute, Center for Earth System Research and Sustainability, University of Hamburg, Germany

[8] Science and Technology Corporation, USA

[9] MetOffice, Hadley Centre, Exeter, UK and AOPP, Department of Physics, Oxford, UK

[10] Space Sciences and Engineering, Boulder, USA

[11] Institute of Applied Physics of the Russian Academy of Science, Nizhny Novgorod, Russia

[12] JPL, California Institute of Technology

[13] Department of Geography, Maynooth University, Ireland

[14] State University of New York at Albany, USA

* **Correspondence to:** Helene Brogniez, LATMOS, IPSL/UVSQ/UPMC/CNRS, Guyancourt 78280, France. helene.brogniez@latmos.ipsl.fr

Atmos. Meas. Tech. Discuss., doi:10.5194/amt-2016-9, 2016
Manuscript under review for journal Atmos. Meas. Tech.
Published: 29 January 2016

Abstract

Several recent studies have observed biases between measurements in the 183.31GHz water vapour line by space-borne sounders and calculations using radiative transfer models with inputs from either radiosondes (RAOBS) or short range forecasts by Numerical Weather Prediction (NWP) models. This paper discusses all the relevant categories of observation-based or model-based data, quantification of their uncertainties, and separation of biases that could be common to all causes from those attributable to a particular cause. Reference observations from radiosondes, Global Navigation Satellite Systems (GNSS), Differential Absorption Lidar (DIAL) and Raman lidar are thus overviewed. Biases arising from their procedures of calibration, NWP models and data assimilation, instrument biases and radiative transfer models (both the models themselves and the underlying spectroscopy) are presented and discussed. Although no single process in the comparisons seems capable of explaining the observed structure of bias, recommendations are made in order to better understand the causes.

1. Introduction

Recent cross-comparisons between the existing satellite microwave sounders of the tropospheric humidity in the 183.31GHz line, SAPHIR (Sondeur Atmospheric du Profil d'Humidité Intertropical par Radiométrie, on Megha-Tropiques), ATMS (Advanced Technology Microwave Sounder, on Suomi-NPP), SSMI/S (Special Sensor Microwave Imager/Sounder, on DMSP-F17 and F18) and MHS (Microwave Humidity Sounder on MetOp-A and B and NOAA-18 and 19), show very good agreement between them, in a 0.3-0.7K range of mean difference, well within the radiometric noises of the instruments [Wilheit et al., 2013; Moradi et al, 2015]. However, when the measurements are compared to radiative transfer model (RTM) calculations using profiles of temperature and humidity either from radiosondes (RAOBS) or from Numerical Weather Prediction (NWP) models, a channel-dependent bias, which increases from the center to the wings of the line, is observed. It was only with the arrival of ATMS and SAPHIR, both launched in October 2011, that the spectral shape of the bias became clear [Clain et al., 2015; Moradi et al., 2015]. Indeed these two instruments sample the 183.31GHz line 5 and 6 times respectively between the line center (providing humidity information for the upper troposphere, above 300hPa) and line wings (for a deeper sounding of the atmosphere) compared to only 3 times for SSMI/S, MHS and AMSU-B (Advanced Microwave Sounding Unit-B that precedeed MHS onboard NOAA 15, 16 and 17). The observed minus calculated brightness temperatures (BTs) are shown in Figure 1, for SAPHIR, ATMS, MHS, SSMI/S against RAOBS or

Atmos. Meas. Tech. Discuss., doi:10.5194/amt-2016-9, 2016
Manuscript under review for journal Atmos. Meas. Tech.
Published: 29 January 2016

NWP systems (Météo-France and European Centre for Medium-range Weather Forecasts) as input for the RTTOV.v11 RTM (Radiative Transfer for the Television InfraRed Observation Satellite (TIROS) Operational Vertical Sounder, [Eyre, 1991; Saunders et al., 1999; Matricardi et al., 2004; Saunders et al., 2013]). It shows a consistent spectrally-dependent bias which is worse further from the line center. Figure 2 presents two maps of the differences between the observed ATMS BTs and the calculated BTs from the all-sky first-guess fields of the ECMWF NWP system for channels 22 (183±1GHz) and 18 (183±7GHz) for a 2-month period. While great differences in areas of snow of persistent thick ice clouds are produced by the RTM's omission of their effect in the simulation of such scenes, there is a clear background difference, between 60°N and 60°S, that increases towards the line wings and that cannot be related to a particular region or atmospheric state.

The importance of knowledge of absolute errors for climate applications (e.g. re-analysis) is clear because these need to detect small changes in the mean state. For real-time NWP, knowing absolute values is less important because observations are bias-corrected, with state-of-the-art NWP systems updating the corrections frequently. Bias corrected observations at 183.31GHz are used widely in NWP models and have important impacts [Geer et al., 2014]. However, the absolute errors in the short-range forecast are also not well known. If sources of systematic errors can be reduced, the need for bias correction would also be reduced, and perhaps one day could be eliminated completely, allowing 183.31GHz observations to become a reference for humidity. This would enable us both to understand better biases in other humidity observations and to improve separation of biases arising from the model (such as cloud cover) from others (such as humidity fields). Bias correction has proven a successful and pragmatic strategy for handling unknown biases, but it does mean we can only correct and characterize the random component of error in model short-range forecasts.

The attribution of the biases requires discussion of all the relevant observational data and model results, quantification of their uncertainties, and separation of biases that could be common to all approaches from those attributable to some particular methodology. Thus we need reference observations from RAOBS, Global Navigation Satellite Systems (GNSS), Differential Absorption Lidar (DIAL) and Raman lidar. We can then attribute biases arising from their calibration procedures, NWP models and data assimilation, instrument biases and RTMs (both the models themselves and the underlying spectroscopy).

If we can successfully attribute the biases then it becomes possible to work on a solution. To illustrate this consider the case of a new observation type for humidity. If we believe that there is a calibration error and we can characterize this error accurately, it may become clear to instrument engineers why the bias exists. If the bias is the sum of ones from a number of sources, this process

Atmos. Meas. Tech. Discuss., doi:10.5194/amt-2016-9, 2016
Manuscript under review for journal Atmos. Meas. Tech.
Published: 29 January 2016

Atmospheric Measurement Techniques Discussions

can't happen. This is also the motivation behind projects such as GAIA-CLIM (Gap Analysis for Integrated Atmospheric ECV - Essential Climate Variable - Climate Monitoring, http://www.gaia-clim.eu/) and FIDUCEO (Fidelity and Uncertainty in Climate Data record from Earth Observations, http://www.fiduceo.eu/), which are also attempting to provide a more accurate assessment of systematic biases in observations.

2. State-of-the-art in observation and modelling

2.1 Reference water vapor measurements

Radiosondes: Uncertainties in relative humidity (RH) measurements by in-situ probes arise mainly from pre-launch calibration procedures, calibration corrections, time-lags and (for some probes) solar radiation heating of the sensor. The GCOS Reference Upper-Air Network (GRUAN, http://www.gruan.org) aims to establish a network of temperature and humidity measurements with traceability to SI standards, and best possible characterization of uncertainties [Dirksen et al., 2014; Bodeker et al., 2015]. For the Vaisala RS92-SGP (hereafter RS92), one of the most common RAOBS probes used operationally and during field campaigns, the GRUAN-characterized uncertainty in RH measurements after correcting known biases is overall below 6%RH, and the only uncorrected bias is a dry bias of ~5%RH at night for temperatures colder than -40°C [Dirksen et al., 2014]. The reliability of the RS92 product in the troposphere has been verified by comparisons with frostpoint hygrometer (FPH) measurements, which are highly accurate balloon-borne humidity measurements, in both tropical and extra-tropical regions. The GRUAN RS92 profile for humidity does not vary greatly from Vaisala's default processing below the upper troposphere (pressures below 200hPa, [Yu et al., 2015]). Further, the most recent intercomparison campaign [Nash et al., 2011] held in Yangjiang (a tropical site in South China) showed good agreement between RS92 and most other operational RAOBS up to the mid-to upper troposphere (pressure above 500hPa), and also with FPH measurements [Vömel et al., 2007]. In the lower to mid-troposphere there is therefore robust agreement and evidence that RAOBS biases could at most be a few percent, with somewhat broader random sampling uncertainties on individual profiles. Also, a given fractional change in humidity causes a considerably small fractional change of BTs. Therefore RAOBS errors could only explain substantial biases near the line center, where the opacity is highest and thus sensitive to water vapor of the upper part of the troposphere, whereas the 183.31GHz biases are the largest towards the wings.

GNSS receivers: GNSS estimates of the atmospheric precipitable water (PW) rely on the measurement of the zenith total delay, the sum of terms due to water vapor (the "wet" delay) and to the dry gases of the troposphere (the "dry" delay). The GNSS-estimated PW has an uncertainty of ~2% in the mean (<1.0mm) [Ning et al., 2015]. However, a recent analysis of the upper-air sounding network deployed during the CINDY/DYNAMO/AMIE field campaign has revealed an unclear, and statistically significant, dry bias in the GNSS values (~2.0mm in PW) in moist conditions for some sites of the campaign [Ciesielski et al., 2014]. Understanding of this dry bias might contribute to the current discussion on the 183GHz bias.

Lidar systems: Two types of lidars can be used to measure water vapor profiles [Behrendt et al., 2007; Bhawar et al., 2011]. Differential absorption lidars (DIAL) measure the water vapor number density with two backscatter signals (at adjacent near-IR wavelengths with high -online- and low -offline- absorption) yielding a self-calibrating system. It only relies on the difference of the water vapor absorption cross-sections σ_{on} and σ_{off} at these two wavelengths (thus eliminating any bias common to both cross-sections). Raman lidars are based on the inelastic scattering by water vapor molecules, and require one instrument-dependent calibration factor for all heights to obtain the mixing ratio. All lidar systems provide data in the cloud-free atmosphere, or until the laser beam reaches an optically thick cloud. Performance simulations as well as intercomparisons have confirmed accuracies < 5% in the troposphere for both systems [Wulfmeyer et al., 2015]. Comparisons between water vapor profiles measured by lidar and by radiosondes further support the accuracy estimates for the global radiosonde data in the troposphere, quoted above.

2.2 Radiative transfer modeling and spectroscopy

Behavior of radiative transfer models: Many cross-comparisons of microwave RTMs have been performed over the years. For instance, Garand et al. (2001) compared different reference and fast models (including RTTOV.v5 and v6 [Saunders et al., 1999]) from the operational NWP community for the 183±1GHz channel. At the time, they found an overall agreement better than 0.5K in BT, which is consistent with the results of Melsheimer et al. (2005), a study dedicated to line-by-line RTMs, with differences within roughly 0.5, 1.5, and 2.5K, respectively for 183±1, ±3, and ±7GHz channels (channels 3 to 5 of MHS). The differences were mainly attributed to the differences in spectroscopy (line parameters and continua) and not the RTMs themselves. This was confirmed by Buehler et al. (2006), who showed that, on average over the globe, the difference between two independent models, RTTOV.v7 and the line-by-line model ARTS (Atmospheric Radiative Transfer Simulator [Buehler et al., 2005a; Eriksson et al., 2011]) is between 0.01K for the 183±1GHz channel and 0.2K for the 183±7GHz channel, except for a few extreme situations. More recently, Chen et al. (2010) have shown that, on a sample of diverse atmospheric profiles, fast and line-by-line RTMs agree within 0.1K for MHS channels, and that this result was highly stable under humid conditions. In their evaluation of SAPHIR using RAOBS, Clain et al. (2015) have shown that the three RTMs RTTOV.v10, ARTS and MonoRTM (Monochromatic Radiative Transfer Model [Clough et al., 2005; Payne et al., 2011]) provide fairly consistent BTs on a common set of tropical profiles, the differences being in the range -1.50K / 0.78K, with the largest differences observed for the central channel (183.31±0.2GHz).

Patterns in the IR are similar in terms of dependence on distance from the line center. Indeed, sensitivity studies on a sample of channels in the 6.3µm water vapor band of the IASI (Infrared Atmospheric Sounding Interferometer) instrument carried out using RTTOV.v11 showed that the difference between calculated and observed BTs increases as the peak altitude of the weighting functions shifts downwards. The same qualitative behavior is observed irrespective of the atmospheric state used in the simulations (i.e. either RAOBS or NWP data). It was also found that, on a purely empirical basis, the pattern of increasing bias can be removed by applying adjustments to the humidity fields input to the simulations (3 to 10% increase below 500hPa) and/or to the strength of the continuum absorption (30% increase in foreign continuum plus a 20% increase of self-continuum). This does not necessarily mean that the same mechanisms must be responsible for the biases observed in the MW radiances, although for the three RTMs mentioned here (RTTOV, ARTS and MonoRTM), the absorption due to the water vapor continuum is parameterized using the same semi-empirical model MT_CKD (MlawerTobin_CloughKneisysDavies, [Mlawer et al., 2012]).

Spectroscopy status: One of the considerations for the accuracy of the line-by-line RT models is the spectroscopic input for the modeling of molecular absorption. The main contributions to the molecular absorption in the MW region of the spectrum are from H_2O, O_2 and N_2, with some minor contributions from O_3 and N_2O. For instance John and Buehler (2004) found that absorption by O_3 corresponds to a decrease of up to 0.5K in the 183±1GHz channel of MHS using ARTS, reaching even smaller values for the other channels. Additional sensitivity tests performed by Clain et al. (2015) using MonoRTM showed that the impact is also marginal in the 183±11GHz channel of SAPHIR (0.05K on average). The details of how the molecular absorption is modeled may vary between different models, but the overall absorption is most commonly calculated for both the contribution near the line centers and the smoothly-varying continuum.

Line parameters (line position and strength, the air-broadened half-width, the self-broadened half-width, the temperature exponent of the width and the pressure shift) may be obtained from laboratory experiments or from theoretical calculations and are collected in databases such as the widely used High Resolution Transmission compilation (HITRAN, [Rothman et al., 2013]). The current edition of HITRAN provides the parameters for Voigt profiles, but future editions of the database will allow for inclusion of additional parameters for more sophisticated line shape models [Tennyson et al., 2014]. Sensitivity tests on Voigt parameters, performed using MonoRTM, have shown that illustrative uncertainties on the foreign (±3%) and self-broadened (±15%) half widths, on the temperature exponent (maximum of 15%) and the pressure shift (maximum of 20%) are certainly too small to explain the observed bias (Payne et al., 2008) and the spectroscopic community (lab and modellers) believes that confidence limits on these parameters are lower than those assumed above. The uncertainty of the dry air absorption including dry continuum and resonance absorption by O_2, O_3, N_2O, NO, CO and other minor atmospheric constituents, as well as uncertainty related to wings of neighboring water lines is not thought to be large enough to account for the observed model-measurement bias.

The physical origin and properties of the water vapor continuum have been debated and probed with measurements for decades. In the current version of the MT_CKD continuum model water vapor contributions are modeled as monomer absorption and the spectral variation of the continuum is assumed to be extremely smooth (sampled every 300GHz in MT_CKD). Figure 3 summarizes comparisons of the continuum coefficients obtained from known laboratory and field (~1km path along the surface, insensitive to vertical distribution of absorbers) measurements (shown by symbols) against the continuum parameters (dotted and dashed lines) that would provide agreement with ground-to-sky radiometric data in MT_CKD. It shows discrepancies (offsets in a log scale) that are not yet understood. There is thus an inconsistency between two large sets of experimental data, namely laboratory together with surface path measurements and radiometric measurements within currently accepted modeling of spectroscopy including both modeling of the continuum and modeling of the atmosphere. This is confirmed by Payne et al. (2011) who concluded that for atmospheric path lengths (looking up) the combination of MPM (Millimeter-wave Propagation Model, [Liebe 1989; Rosenkranz, 1998]) foreign and self-continuum (solid lines in Figure 3) is inconsistent with the radiometric measurements at high column water vapor amounts.

Atmos. Meas. Tech. Discuss., doi:10.5194/amt-2016-9, 2016
Manuscript under review for journal Atmos. Meas. Tech.
Published: 29 January 2016

Atmospheric Measurement Techniques Discussions

Finally recent laboratory studies have resulted in unambiguous detection of H_2O dimer absorption in the millimeter-wave range [Tretyakov et al., 2013; Serov et al., 2014] and to the development of a model to describe it [Odintsova et al., 2014]. This absorption shows spectral variation on scales that are not accounted for in the current version of MT_CKD or in Liebe-based models. Odintsova et al. (2014) indicate that the inclusion of dimer absorption can result in small-scale spectral (~1GHz) variation of 0.5 to 1K in up-looking (ground-based) spectra. The impact of accounting for dimer absorption on RT modeling for the 183.31GHz satellite radiometer channels has yet to be determined.

2.3 Water vapor analysis

In NWP models, the main observation types influencing humidity analyses are in-situ data like RAOBS and remote sensing observations from IR and MW sensors [Andersson et al., 2005]. Cai and Kalnay (2005) have illustrated how a balance can arise between a forecast model (subject to a inherent bias with respect to the truth) and observations (with different bias characteristics). Variational Bias Correction (VarBC) techniques have been developed to adaptively estimate, as part of the constrained optimization that also provides the best estimate of the latest atmospheric state, a bias correction for each of the various assimilated observations [Dee, 2005; Auligné et al., 2007]. In order to anchor the bias corrections and the final humidity analysis, RAOBS are not bias corrected with VarBC (although corrections are applied to standardize them to night-time RS92 observations: Agusti-Panareda et al. 2009). Hence it is possible that humidity analyses share similar biases to radiosondes, which might explain some of the consistency between the channel-dependent bias found with both in-situ measurements and NWP simulations. More investigations would be needed to test the impact of this anchoring, although it is expected from the discussion in Section 2.1 that the effect would be more pronounced in the upper-tropospheric channels (close to the line center) than in the lower tropospheric channels (in the line wings).

An issue that affects most comparisons between 183.31GHz observations and a reference is cloud detection. Indeed clouds and precipitation are not usually included in MW radiative transfer simulations, while they naturally reduce 183.31GHz BTs, particularly in the lower-peaking channels (see for instance the negative bias in the Inter-Tropical Convergence Zone in Figure 2), either by scattering or by absorption, which shifts upwards the altitude of the weighting function. There are major sources of uncertainty in modeling the effects of cloud and precipitation around the 183.31GHz line, coming from the difficulty in specifying shape, density, and particle size distribution of solid precipitating particles [Burns et al., 1997; Doherty et al., 2007; Geer and Baordo, 2014]. However, if the model cloud and precipitation fields were unbiased compared to reality, a negative first guess departure in a 183.31GHz channel would indicate that the observation selection is too cloudy (i.e. cold). This would be consistent with a cloud detection that is missing some cloud-affected scenes.

Different cloud screening methods are applied depending on the sensor and the channels available, leading to different accuracies of the cloud screening. For instance, ATMS offers a large suite of channels that can complement each other to separate clear and cloudy scenes [Bormann et al., 2013], while SAPHIR provides only channels in the 183.31GHz line, giving fewer possibilities for cloud detection [Chambon et al., 2015]. Several filtering techniques using only 183.31GHz channels exist and rely on the strong reduction in BT induced by scattering and/or absorption, which can reach up to 20K in regions of intense convection [Greenwald and Christopher, 2002; Hong et al., 2005; Buehler et al., 2007]. However, it is difficult to screen all clouds, so residual biases may be present. The all-sky first guess departures from assimilation at ECMWF [e.g. Geer et al., 2014] are the only routinely computed differences in the 183.31GHz line which attempt to take into account the effects of cloud and precipitation in the radiative transfer modeling. Compared to those differences computed using clear-sky radiative transfer and cloud-screening (which are shown in Figure 1 marked "ECMWF"), the all-sky ATMS biases are smaller by 0.4K in the ±7 GHz channel, suggesting some but not nearly all of the bias in the lower peaking channels can be explained by residual cloud effects.

2.4 Space-borne microwave radiometers

Intercomparison of instruments: Ways to compare measurements by different satellite instruments include the simultaneous-nadir-overpasses technique (limiting the comparisons to the highest latitudes, [John et al., 2012]) and the use of "natural targets" that have very little variability or the averaging over a lot of scenes [John et al., 2013a]. Another technique is the double difference technique that uses NWP fields input to a RTM as a transfer function between two radiometers that have few common overpasses. Using this technique, recent comparisons of the 183.31GHz channel calibrations have been performed by the Global Precipitation Mission (GPM) intercalibration working group, or (XCAL team). Mean differences between the GMI (GPM Microwave Imager) BTs and the four operational MHS sensors onboard MetOp-A, MetOp-B, NOAA-18, and NOAA-19 as well as the Suomi NPP ATMS and Megha-Tropiques SAPHIR instruments are given in Table 2.

Calibration issues: Since GPM is in a precessing orbit with an inclination of 65°, it frequently crosses the orbits of the other sounders providing near coincident observations several times each day in the 65°N/65°S belt. Post launch, a series of GPM calibration maneuvers was performed, and the resulting data were used to develop corrections for magnetic-induced biases, cross-track biases and updates to the pre-launch spillover corrections, as well as to verify the channel polarizations. The resulting GMI calibration is based on the data from these calibration maneuvers and does not depend on RTM. The GMI calibration is also completely independent of the calibration of the MHS, ATMS, and SAPHIR instruments, thus providing a useful measure of the absolute calibration accuracy of the 183.31GHz channels for these sensors. The differences in Table 2 show consistent results, with values within 1K for all channels and all sensors. Errors in the calibration of the SSMI/S 183.31GHz channels are substantially larger due to substantial biases caused by reflector emission and solar intrusion issues [Berg and Sapiano, 2013].

Scan asymmetry: Cross-track scanners sometimes show asymmetries across the swath, indicating issues related to the imperfectly known antenna pattern, which often evolve with the age of the instruments. Far from nadir, channels sounding deep into the troposphere, located on the wings of the 183.31GHz line, might be more affected by antenna issues than higher peaking channels, located in the center of the line, due to radiation measured by the side-lobes. Such asymmetries were found for AMSU-B and MHS [Buehler et al., 2005b; John et al., 2013b] but so far the monitoring of SAPHIR has not shown any scan-asymmetry. For ATMS, comparisons of Temperature Data Records (TDR, calibrated antenna temperatures) and Sensor Data Records (SDR, BT after further applying beam efficiency and scan position dependent bias corrections) for the 183.31GHz channels show the same behavior meaning that the TDR to SRD conversion is not responsible for the bias, although it seems to introduce some dependence on the viewing angle that warrants further investigation. For other sensors, in particular AMSU-B and MHS this has so far not been thoroughly investigated, partly due to a lack of publicly available pre-launch measurements of antenna pattern.

3. Recommendations

On the reference measurements: Research on better characterization of uncertainties of the Vaisala RS92 measurements, and on offline corrections of biases, indicate that the remaining RAOBS biases could only explain discrepancies in the center of the 183.31GHz line, not in its wings. Nevertheless cross-comparisons of water vapor measured by lidars and RAOBS and simulated by NWP models

Atmos. Meas. Tech. Discuss., doi:10.5194/amt-2016-9, 2016
Manuscript under review for journal Atmos. Meas. Tech.
Published: 29 January 2016

are strongly encouraged in order to confirm the spectral pattern of the 183.31GHz bias. Finally the next WMO upper-air intercomparison campaign is strongly encouraged to include the new Vaisala RS41 probes, which are likely to be even more accurate than the RS92.

On the radiative transfer and the spectroscopy: For the purposes of atmospheric remote sensing, consistency with in-situ atmospheric radiometric measurements is key. Currently, the cause of the apparent discrepancy between the laboratory measurements and the atmospheric results remains an open question. Continuation and augmentation of laboratory measurements are strongly encouraged to check the uncertainty levels for the main spectroscopic parameters, and to explore new line shape parametrizations. Also, the use of ground based 183.31GHz instruments can help to better constrain the parametrizations, because the surface does not contaminate the measurements. In particular measurements at high values of precipitable water (> 3cm) are required to constrain the self-broadened continuum. For instance, recent opacity measurements performed with the radio occultation active spectrometer ATOMMS (Active Temperature Ozone Moisture Microwave Spectrometer, [Kursinski et al., 2012]) have shown two spectral discrepancies. The first discrepancy is a poor match between the Liebe MPM93 model and the measured line shape within 4 GHz of the 183.31GHz line center. In this interval, the HITRAN-based AM6.2 model of Scott Paine (Harvard-Smithonian Center for Astrophysics) matches the measurements very well, to 0.3%. However, there is a significant spectral discrepancy in the wing of the line with respect to the AM6.2 modeled opacity, which is apparently lower than the measured opacity. Viewed from space, this would translate into a modeled BT that is higher than measured (the modeled radiation coming from deeper in the atmosphere). Detailed understanding requires additional measurements and more quantitative examination. In particular it is recommended that ATOMMS measurements be made from aircraft at a range of pressures in order to determine the true line shape variation with pressure.

Better coordination between instrument and calibration experts and RT modelers would also help to ensure that RT simulations are consistent with the most recent spectroscopy measurements.

On the water vapor analysis: The two main approaches to handling clouds (avoiding observations affected by cloud - the « clear-sky » approach; or using model cloud-fields and analysing all data - the « all-sky » approach) give similar but not identical biases. Accordingly, the method for handling clouds can only explain part of the bias, but further investigation is needed to determine more precisely the impact on the size and characteristics of the bias. Testing the impact of the RAOBS constraint in the bias correction schemes of NWP systems with respect to the various observing systems (MW, IR, GNSS) should be also performed.

On the space-borne sounders: The instrument spectral response functions (SRF) are too often averaged over the pass bands and assumed to be rectangular when unknown. Therefore the pre-launch recording and permanent availability of digital data and metadata of SRF and antenna patterns are strongly encouraged for future instruments. Moreover, in the future, it is considered likely that Radio Frequency Interference (RFI) may become a threat at 183 GHz. It is therefore important both to measure the bandpasses of the instrument accurately, and also to ensure there is no sensitivity to bands outside the protected frequency. This point reinforces the need to have (an easy) access to the SRF of each instrument, as well as the conversion procedures between counts/radiances/BT. Finally, biases arising from asymmetric effects for channels with widely spaced double-side bands, as SAPHIR does, may also have an impact on the spectral characteristics of the bias. The size and nature of this asymmetry needs to be accurately documented.

Acknowledgments

This paper reflects the outcomes of a workshop that was held 29-30 June 2015, in Paris. The process of identifying the key questions was performed during a series of working group sessions whose additional participants are thanked: C. Accadia, R. Armante, P. Brunel, J. Bureau, M. Dejus, S. Di Michele, A. Doherty, C. Dufour, F. Duruisseau R. Fallourd, C. Goldstein, B. Ingleby, E. Kim, S. Laviola, A. Martini, V. Mattioli, L. Picon, C. Prigent, P. Sinigoj, N. Viltard. We warmly thank the CNES and Megha-Tropiques for the financial support of the workshop and also Sophie Cloché (IPSL) for her immense help in its organization.

Atmos. Meas. Tech. Discuss., doi:10.5194/amt-2016-9, 2016
Manuscript under review for journal Atmos. Meas. Tech.
Published: 29 January 2016

Atmospheric Measurement Techniques Discussions

References

Andersson E., P. Bauer, A. Beljaars, F. Chevallier, E. Holm, M. Janiskova, P. Kallberg, G. Kelly, P. Lopez, A. McNally, E. Moreau, A. Simmons, J-N Thépaut and A. Tompkins (2005), Assimilation and modeling of the atmospheric hydrological cycle in the ECMWF forecasting system. Bull. Amer. Meteor. Soc. doi: 10.1175/BAMS-86-3-387, 387-402.

Agustí-Panareda, A., Vasiljevic, D., Beljaars, A., Bock, O., Guichard, F., Nuret, M., Garcia Mendez, A., Andersson, E., Bechtold, P., Fink, A., Hersbach, H., Lafore, J.-P., Ngamini, J.-B., Parker, D. J., Redelsperger, J.-L. and Tompkins, A. M. (2009), Radiosonde humidity bias correction over the West African region for the special AMMA reanalysis at ECMWF. Q. J. R. Meteorol. Soc., 135, 595–617, doi:10.1002/qj.396.

Auligné, T., McNally, A. P. and Dee, D. P. (2007), Adaptive bias correction for satellite data in a numerical weather prediction system. Q. J. R. Meteorol. Soc., 133, 631–642, doi:10.1002/qj.56.

Bauer A. Godon M., Carlier J., Ma Q., Tipping R.H. (1993), Absorption by H_20 and H_20-N_2 mixtures at 153 GHz, J. Quant. Spectrosc. Radiat. Transfer, 50, 463-475.

Bauer A., Godon M., Carlier J., Ma. Q. (1995), Water vapor absorption in the atmospheric window at 239 GHz, J. Quant. Spectrosc. Radiat.Transfer, 53, 411-423.

Berg, W. and M. Sapiano (2013), Corrections and APC for SSMIS, Technical report, Colorado State University [Available online at http://rain.atmos.colostate.edu/FCDR/doc/CSU_FCDR_ssmis_corrections_tech_report.pdf].

Behrendt A., and co-authors (2007), Intercomparison of water vapor data measures with lidar during IHOP_2002. Part I: Airborne to ground-based lidar systems and comparisons with chilled-mirror hygrometer radiosondes. J. Atmos. Oceanic Technol., 24, pp 3-21, doi:10.1175/JTECH1924.1.

Bhawar R. and co-authors (2011), The water vapour intercomparison effort in the framework of the Convective and Orographically-induced Precipitation Study: airborne-to-ground-based and airborne-to-airborne lidar systems. Q. J. R. Meteorol. Soc., 137, 325-348, doi:10.1002/qj697.

Bodeker G., S. Bojinski, D. Cimini, R. Dirksen, M. Haeffelin, J. Hannigan, D. Hurst, T. Leblanc, F. Madonna, M. Maturilli, A. Mikalsen, R. Philipona, T. Reale, D. Seidel, D. Tan, P. Thorne, H. Vömel and J. Wang (2015), Reference upper-air observations for climate: From concept to reality. Bull. Amer. Meteor. Soc. doi:10.1175/BAMS-D-14-00072.1, in press.

Atmos. Meas. Tech. Discuss., doi:10.5194/amt-2016-9, 2016
Manuscript under review for journal Atmos. Meas. Tech.
Published: 29 January 2016

Atmospheric Measurement Techniques
Open Access
Discussions

Bormann, N., A. Fouilloux, and W. Bell (2013), Evaluation and assimilation of ATMS data in the ECMWF system, J. Geophys. Res. Atmos., 118, 12,970–12,980, doi:10.1002/2013JD020325.

Buehler, S. A., P. Eriksson, T. Kuhn, A. von Engeln and C. Verdes (2005a), ARTS, the Atmospheric Radiative Transfer Simulator, J. Quant. Spectrosc. Radiat. Transfer, 91(1), 65-93, doi:10.1016/j.jqsrt.2004.05.051.

Buehler, S. A., M. Kuvatov, and V. O. John (2005b), Scan asymmetries in AMSU-B data, Geophys. Res. Lett., 32, L24810, doi:10.1029/2005GL024747.

Buehler, S. A., N. Courcoux, and V. O. John (2006), Radiative transfer calculations for a passive microwave satellite sensor: Comparing a fast model and a line-by-line model. J. Geophys. Res., 111, D20304, doi:10.1029/2005JD006552.

Buehler, S. A., M. Kuvatov, T. R. Sreerekha, V. O. John, B. Rydberg, P. Eriksson, and J. Notholt (2007), A cloud filtering method for microwave upper tropospheric humidity measurements, Atmos. Chem. Phys., 7(21), 5531–5542, doi:10.5194/acp-7-5531-2007.

Burns, B., Wu, X., Diak, G. (1997), Effects of precipitation and cloud ice on brightness temperatures in AMSU moisture channels. IEEE Trans. Geosci. Remote Sens. 35, 1429–1437.

Cai M. and E. Kalnay (2005), Can reanalysis have anthropogenic climate trends without model forcing ? J. Clim., 18, 1844-1849, doi:10.1175/JCLI3347.1.

Chambon, P., Meunier, L.-F., Guillaume, F., Piriou, J.-M., Roca, R. and Mahfouf, J.-F. (2015), Investigating the impact of the water-vapour sounding observations from SAPHIR on board Megha-Tropiques for the ARPEGE global model. Q. J. R. Meteorol. Soc., 141: 1769–1779. doi:10.1002/qj.2478.

Chen Y., Y. Han, P. Van Delst and F. Weng (2010), On water vapor jacobian in fast radiative transfer model, J. Geophys. Res., 115, D12303, doi:10.1029/2009JD013379.

Ciesielski P. E., H. Yu, R. H. Johnson, K. Yoneyama, M. Katsumata, C. N. Long, J. Wang, S. M. Loehrer, K. Young, S. F. Williams, W. Brown, J. Braun, and R. Van Hove (2014), Quality-controlled upper-air sounding dataset for DYNAMO/CINDY/AMIE: development and corrections. J. Atmos. Oceanic Technol., 31, 741-764, doi:10.11175/JTECH-D-13-00165.1.

Clain G., H. Brogniez, V. H. Payne, V. O. John and M. Luo (2015), An assessment of SAPHIR calibration using high quality tropical soundings. J. Atmos. Oceanic Technol., 32 (1), pp.61-78, doi: 10.1175/JTECH-D-14-00054.1.

Atmos. Meas. Tech. Discuss., doi:10.5194/amt-2016-9, 2016
Manuscript under review for journal Atmos. Meas. Tech.
Published: 29 January 2016

Clough S., M. Shephard, E. Mlawer, J. Delamere, M. Iacono, K. Cady-Pereira, S. Boukabara, P. Brown (2005), Atmospheric radiative transfer modelling: a summary of the AER codes, J. Quant. Spectrosc. Radiat. Transfer, 91(2), 233-244, doi:10.1016j/j.jqsrt.2004.05.058.

Dee D.P. (2005), Bias and data assimilation. Q. J. R. Meteorol. Soc. 131: 3323–3343.

Dirksen, R. J., M. Sommer, F. J. Immler, D. F. Hurst, R. Kivi, and H. Vömel (2014), Reference quality upper-air measurements: GRUAN data processing for the Vaisala RS92 radiosonde, Atmos. Meas. Tech., 7, 4463-4490, doi:10.5194/amt-7-4463-2014.

Doherty, A., T.R. Sreerekha, U. M. O'Keeffe and S. J. English (2007), Ice hydrometeor microphysical assumptions in radiative transfer models at AMSU-B frequencies, Q. J. R. Meteorol. Soc., 133, 1205-1212.

Eyre J. R. (1991), A fast radiative transfer model for satellite sounding systems. ECMWF Research Dept. Tech. Memo. 176 (available from ECMWF).

Eriksson, P., S. A. Buehler, C. P. Davis, C. Emde, and O. Lemke (2011), ARTS, the atmospheric radiative transfer simulator, Version 2. J. Quant. Spectrosc. Radiat. Transfer, 112(10), 1551–1558, doi:10.1016/j.jqsrt.2011.03.001.

Garand, L., et al. (2001), Radiance and jacobian intercomparison of radiative transfer models applied to HIRS and AMSU channels. J. Geophys. Res., 106(D20), 24,017–24,031.

Geer A. J. and F. Baordo (2014), Improved scattering radiative transfer for frozen hydrometeors at microwave frequencies. Atmos. Meas. Tech., 7, 1839-1860, doi:10.5194/amt-7-1839-2014.

Geer A.J., F. Baordo, N. Bormann, S. English (2014), All-sky assimilation of microwave humidity sounders. ECMWF technical memorandum 741 [available at www.ecmwf.int].

Godon, M., Carlier J., Bauer A. (1992), Laboratory studies of water vapor absorption in the atmospheric window at 213 GHz. J. Quant. Spectrosc. Radiat. Transfer, 47, 275-285.

Greenwald, T. J. and Christopher, S. A.: Effect of cold clouds on satellite measurements near 183 GHz, J. Geophys. Res., 107, 4170, doi:10.1029/2000JD0002580, 2002.

Hong, G., Heygster, G., Miao, J., and Kunzi, K.: Detection of tropical deep convective clouds from AMSU-B water vapor channels measurements, J. Geophys. Res., 110, doi:10.1029/2004JD004949, 2005.

Immler, F. J., J. Dykema, T. Gardiner, D. N. Whiteman, P. W. Thorne, and H. Vömel (2010), Reference Quality Upper-Air Measurements: guidance for developing GRUAN data products. Atm. Meas. Tech., 3, 1217–1231, doi:10.5194/amt-3-1217-2010.

John, V. O. and S. A. Buehler (2004), The impact of ozone lines on AMSU-B radiances, Geophys. Res. Lett., 31, L21108, doi:10.1029/2004GL021214.

John, V. O., G. Holl, S. A. Buehler, B. Candy, R. W. Saunders, and D. E. Parker (2012), Understanding inter-satellite biases of microwave humidity sounders using global simultaneous nadir overpasses, J. Geophys. Res., 117(D2), D02305, doi:10.1029/2011JD016349.

John, V. O., R. P. Allan, B. Bell, S. A. Buehler, and A. Kottayil (2013a), Assessment of inter-calibration methods for satellite microwave humidity sounders, J. Geophys. Res., 118, 4906–4918, doi:10.1002/jgrd.50358.

John, V. O., G. Holl, N. Atkinson, and S. A. Buehler (2013b), Monitoring scan asymmetry of microwave humidity sounding channels using simultaneous all angle collocations (SAACs), J. Geophys. Res., 118, 1536–1545, doi:10.1002/jgrd.50154.

Katkov V. Yu., Sverdlov B.A., Furashov N.I. (1995) Experimental estimates of the value and temperature dependence of the air-humidity quadratic component of the atmospheric water-vapor absorption coefficient in the frequency band of 140-410 GHz. Radiophysics and Quantum Electronics, 38(12) 835-844.

Koshelev M.A., Serov E.A., Parshin V.V., Tretyakov M.Yu. (2011), Millimeter wave continuum absorption in moist nitrogen at temperatures 261 – 328 K, J. Quant. Spectrosc. Radiat. Transfer, 112, 2704–2712.

Kuhn T., Bauer A., Godon M., Buehler S., Kunzi K. (2002), Water vapor continuum: absorption measurements at 350 GHz and model calculations. J. Quant. Spectrosc. Radiat. Transfer, 74 545–562.

Kursinski E. R., D. Ward, M Stovern, A. Otarola, A. Young, B. Wheelwright, R. Stickney, S. Albanna, B. Duffy, C. Groppy and J. Hainsworth (2012), Development and testing of the Active Temperature, Ozone and Moisture Microwave Spectrometer (ATOMMS) cm and mm wavelength occultation instrument, Atm. Meas. Tech., 5, 439-456, doi:10.5194/amt-5-439-2012.

Liebe H.J. (1984), The atmospheric water vapor continuum below 300 GHz. lnt. J. Infrared Millimeter Waves. 5(2), 207-227.

Liebe H.J., Layton D.H. (1987), Millimeter-wave properties of the atmosphere: Laboratory studies and propagation modeling, NTIA Rep. 87-224, Natl. Telecommun. and Inf. Admin., Boulder, Colo.

Liebe H.J (1989), MPM- An atmospheric Millimeter wave Propagation Model, Int. J. Infrared Millimeter waves, 10, 631-650

Matricardi M., F. Chevallier, G. Kelly and J-N Thépaut (2004), An improved general fast radiative transfer model for the assimilation of radiance observations, Q. J. R. Meteorol. Soc., 130, 153-173, doi:10.1256/qj.02.181.

Melsheimer, C., C. Verdes, S. A. Buehler, C. Emde, P. Eriksson, D. G. Feist, S. Ichizawa, V. O. John, Y. Kasai, G. Kopp, N. Koulev, T. Kuhn, O. Lemke, S. Ochiai, F. Schreier, T. R. Sreerekha, M. Suzuki, C. Takahashi, S. Tsujimaru, and J. Urban (2005), Intercomparison of general purpose clear sky atmospheric radiative transfer models for the millimeter/submillimeter spectral range. Radio Sci., RS1007, doi:10.1029/2004RS003110.

Mlawer E., V. Payne, J-L Moncet, J. Delamere, M. Alvarado and D. Tobin (2012), Development and recent evaluation of the MT_CKD model of continuum absorption, Phil. Trans. R. Soc. A (370, 2520-2556, doi:10.1098/rsta.2011.0295.

Moradi I., R. R. Ferraro, P. Eriksson and F. Weng (2015), Intercalibration and validation of observations from ATMS and SAPHIR microwave sounders. IEEE Trans. Geosc. Rem. Sens., doi: 10.1109/TGRS.2015.2427165.

Nash J., T. Oakley, H. Vömel and L. Wei (2011), WMO intercomparison of high quality radiosonde systems, Yangjiang, China, 12 July -3 August 2010. WMO Tech. Doc. WMO/TD1580, Instruments and Observing Methods Rep. 107, 238 pp.

Ning, T., J. Wang, G. Elgered, G. Dick, J.Wickert, M. Bradke, M. Sommer, R. Querel, and D. Smale, 2015: The uncertainty of the atmospheric integrated water vapour estimated from GNSS observations. *Atmos. Measurement Tech.*, in press.

Odintsova T., M. Tretyakov, A. F. Krupnov, C. Leforestier (2014), The water dimer millimeter-wave spectrum at ambient conditions: A simple model for practical applications, J. Quant. Spectrosc. Radiat. Transfer, 140, 75-80, doi: 10.1016/j/jqsrt.2014.02.016.

Atmos. Meas. Tech. Discuss., doi:10.5194/amt-2016-9, 2016
Manuscript under review for journal Atmos. Meas. Tech.
Published: 29 January 2016

Atmospheric Measurement Techniques Discussions
Open Access
EGU

Payne V., J. Delamere, K. Cady-Pereira, R. Gamache, J-L Moncet, E. Mlawer and S. Clough (2008), Air-broadened half-widths of the 22- and 183-GHz water vapor lines, IEEE Trans. Geosci. Remote Sens., 46(11), 3601-3617, doi:10.1109/TGRS.2008.2002435.

Payne V., E. Mlawer, K. Cady-Pereira and J-L Moncet (2011), Water vapour continuum absorption in the microwave, IEEE Trans. Geosci. Remote Sens., 49(6), 2194-2208, doi:10.1109/TGRS.2010.2091416.

Rothman L. S. and co-authors (2013), The HITRAN2012 molecular spectroscopic database, J. Quant. Spectrosc. Radiat. Transfer, 130, 4-50.

Rosenkranz P. (1998), Water vapor microwave continuum absorption: a comparison of measurements and models, Radio Science, 33 (4), 919-928.

Rosenkranz P.W. (1999), Correction to "Water vapor microwave continuum absorption: A comparison of measurements and models". Radio Science, 34(4) 1025.

Saunders, R., M. Matricardi, and P. Brunel (1999), An improved fast radiative transfer model for assimilation of satellite radiance observations. Q. J. R. Meteorol. Soc., 125, 1407–1425.

Saunders R., J. Hocking, D. Rundle, P. Rayer, M. Matricardi, A. Geer, C. Lupu, P. Brunel, J. Vidot (2013), RTTOV-11: Science and validation report. NWP-SAF report, Met Office, UK, 62pp.

Serov E. A., M. A. Koshelev, T. A. Odintsova, V. V. Parshin and M. Tretyakov (2014), Rotationally resolved water dimer spectra in atmospheric air and pure water in the 188-258 GHz range, Phys. Chem. Chem. Phys, 16, 26221.

Tennyson J, Bernath PF, Campargue A, Csaszar AG, Daumont L, Gamache RR, Hodges JT, Lisak D, Naumenko OV, Rothman LS, Tran H, Zobov NF, Buldyreva J, Boone CD, De Vizia MD, Gianfrani L, Hartmann JM, McPheat R, Weidmann D, Murray J, Ngo NH, Polyansky OL (2014), Recommended isolated-line profile for representing high-resolution spectroscopic transitions. Pure Appl. Chem., 86, 1931-1943.

Tretyakov M. , E. A. Serov, M. A. Koshelev, V. V. Parshin and A. F. Krupnov (2013), Water dimer rotationally resolved millimeter-wave spectrum observation at room temperature, Physical Review Letters, 110, 093001.

Turner D.D., Cadeddu M.P., Löhnert U., Crewell S., Vogelmann A.M. (2009), Modifications to the water vapor continuum in the microwave suggested by ground-based 150-GHz observations. IEEE Trans. Geosci. Rem. Sens., 47(10) 3326-3337.

Vömel H. , H. Selkirk, L. Miloshevich, J. Valverde-Canossa, J. Valdés, E. Kyrö, R. Kivi, W. Stolz, G. Peng, and J. A. Diaz (2007), Radiation dry bias of the Vaisala RS92 humidity sensor. *J. Atmos. Oceanic Technol*., **24**, 953–963. doi: http://dx.doi.org/10.1175/JTECH2019.1.

Wilheit T. H. Brogniez, S. Datta, W. Linwood Jones, V. Payne, E. Stokcer and J. Wang (2013), The use of SAPHIR on Megha-Tropiques for intercalibration of polar-orbiting microwave water vapor sounders. 2013 EUMETSAT meteorological satellite Conference / 19th AMS Satellite Meteorology Oceanography and Climatology Conference, Vienna, Austria, 272. [Available online at www.eumetsat.int/website/wcm/idc/idcplg?IdcService=GET_FILE&dDocName=PDF_CONF_2013_ABSTRACTS&RevisionSelectionMethod=LatestReleased&Rendition=Web.]

Wulfmeyer V., R. Hardesty, D. Turner, A. Behrendt, M. Cadeddu, P. Di Girolamo, P. Schlüssel, J. Van Baelen and F. Zus (2015), A review of the remote sensing of lower tropospheric thermodynamic profiles and its indispensable role for the understanding and the simulation of water and energy cycles. Rev. Geophys., 53, doi :10.1002/2014RG000476.

Yu H., P. E. Ciesielski, J. Wang, H-C Kuo, H. Vömel, and R. Dirksen, (2015), Evaluation of humidity correction methods for Vaisala RS92 tropical sounding data. J. Atmos. Oceanic Technol., 32, 397–411, doi:10.1175/JTECH-D-14-00166.1.

Atmos. Meas. Tech. Discuss., doi:10.5194/amt-2016-9, 2016
Manuscript under review for journal Atmos. Meas. Tech.
Published: 29 January 2016

Tables

Table 1: List of satellites, sensors and their channels located in the f_0= 183.31 GHz absorption line

Satellite	Instrument	Scanning geometry, maximum satellite zenith angle (θ_{zen}, in °), swath width (km) and number of pixels/samples per scan line	Channels around f_0= 183.31 GHz (GHz)	Bandwidth (MHz)	In-flight NeDT (K)
Megha-Tropiques	SAPHIR	cross-track $\theta_{zen} = \pm 50.7°$ swath width = 1700 km 130 contiguous pixels	$f_0 \pm 0.2$	200	1.44
			$f_0 \pm 1.1$	350	1.05
			$f_0 \pm 2.8$	500	0.91
			$f_0 \pm 4.2$	700	0.77
			$f_0 \pm 6.8$	1200	0.63
			$f_0 \pm 11.0$	2000	0.54
Suomi-NPP	ATMS	cross-track $\theta_{zen} = \pm 64°$ swath width = 2503 km 96 samples	$f_0 \pm 1.0$	500	0.9
			$f_0 \pm 1.1$	1000	0.8
			$f_0 \pm 2.8$	1000	0.8
			$f_0 \pm 4.2$	2000	0.8
			$f_0 \pm 7.0$	2000	0.8
MetOp-A / B NOAA-18 / 19	MHS	cross-track $\theta_{zen} = \pm 50°$ swath width = 1920 km 90 contiguous pixels	$f_0 \pm 1.0$	500	1.06
			$f_0 \pm 3.0$	1000	0.70
			$f_0 + 7.0$	2200	0.84
DMSP F17 / F18	SSMI/S	conical $\theta_{zen} = 53.1°$ swath width = 1707 km 180 samples	$f_0 \pm 1.0$	513	0.81
			$f_0 \pm 3.0$	1019	0.67
			$f_0 \pm 6.6$	1526	0.97

Atmos. Meas. Tech. Discuss., doi:10.5194/amt-2016-9, 2016
Manuscript under review for journal Atmos. Meas. Tech.
Published: 29 January 2016

Atmospheric Measurement Techniques Discussions

Table 2: Mean calibration differences versus the GPM GMI radiometer for the cross-track sounders listed in Table 1 (GMI – sounder) for channels near the f_0=183.31 GHz absorption line, computed by the GPM XCAL intercalibration team.

Satellite	Instrument	High frequency channels around f_0= 183.31 GHz (GHz)	Calibration difference (K)
Megha-Tropiques	SAPHIR	$f_0 \pm 0.2$	0.18
		$f_0 \pm 1.1$	-0.56
		$f_0 \pm 2.8$	-0.42
		$f_0 \pm 4.2$	-0.66
		$f_0 \pm 6.8$	-0.32
		$f_0 \pm 11.0$	-0.41
Suomi-NPP	ATMS	$f_0 \pm 1.0$	0.40
		$f_0 \pm 1.8$	-0.30
		$f_0 \pm 3.0$	-0.97
		$f_0 \pm 4.5$	-0.82
		$f_0 \pm 7.0$	-0.78
MetOp-A	MHS	$f_0 \pm 1.0$	0.66
		$f_0 \pm 3.0$	-0.17
		$f_0 + 7.0$	-0.14
MetOp-B	MHS	$f_0 \pm 1.0$	0.60
		$f_0 \pm 3.0$	0.00
		$f_0 + 7.0$	0.09
NOAA-18	MHS	$f_0 \pm 1.0$	0.24
		$f_0 \pm 3.0$	-0.12
		$f_0 + 7.0$	-0.06
NOAA-19	MHS	$f_0 \pm 1.0$	0.94
		$f_0 \pm 3.0$	0.03
		$f_0 + 7.0$	-0.05

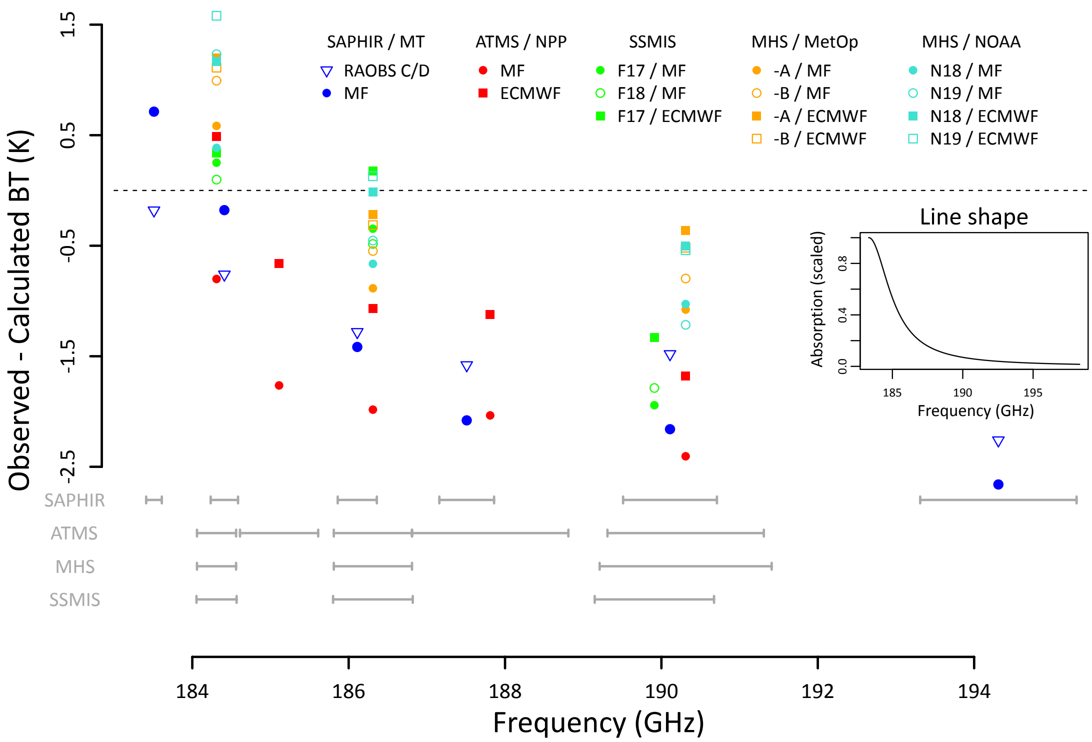

Figure 1: Mean observed minus calculated BT. All the calculated BTs are from RTTOVv11 run on RAOBS measurements (triangles) or Météo-France NWP profiles (MF, circles) or European Centre for Medium-range Weather Forecasts NWP profiles (ECMWF, squares). Each color refers to a specific sensor, as in the legend and the horizontal gray bars indicate the width of the band passes. The RAOB measurements were collected during the Cooperative Indian Ocean Experiment on Intraseasonal Variability (CINDY)/Dynamics of the Madden-Julian Oscillation (DYNAMO)/ARM Madden-Julian Oscillation (MJO) Investigation Experiment (AMIE) field campaign, winter 2011-2012. The inset is a scaled representation of the 183GHz line, assuming a Van Vleck-Weisskopf shape.

Atmos. Meas. Tech. Discuss., doi:10.5194/amt-2016-9, 2016
Manuscript under review for journal Atmos. Meas. Tech.
Published: 29 January 2016

Atmospheric Measurement Techniques Discussions

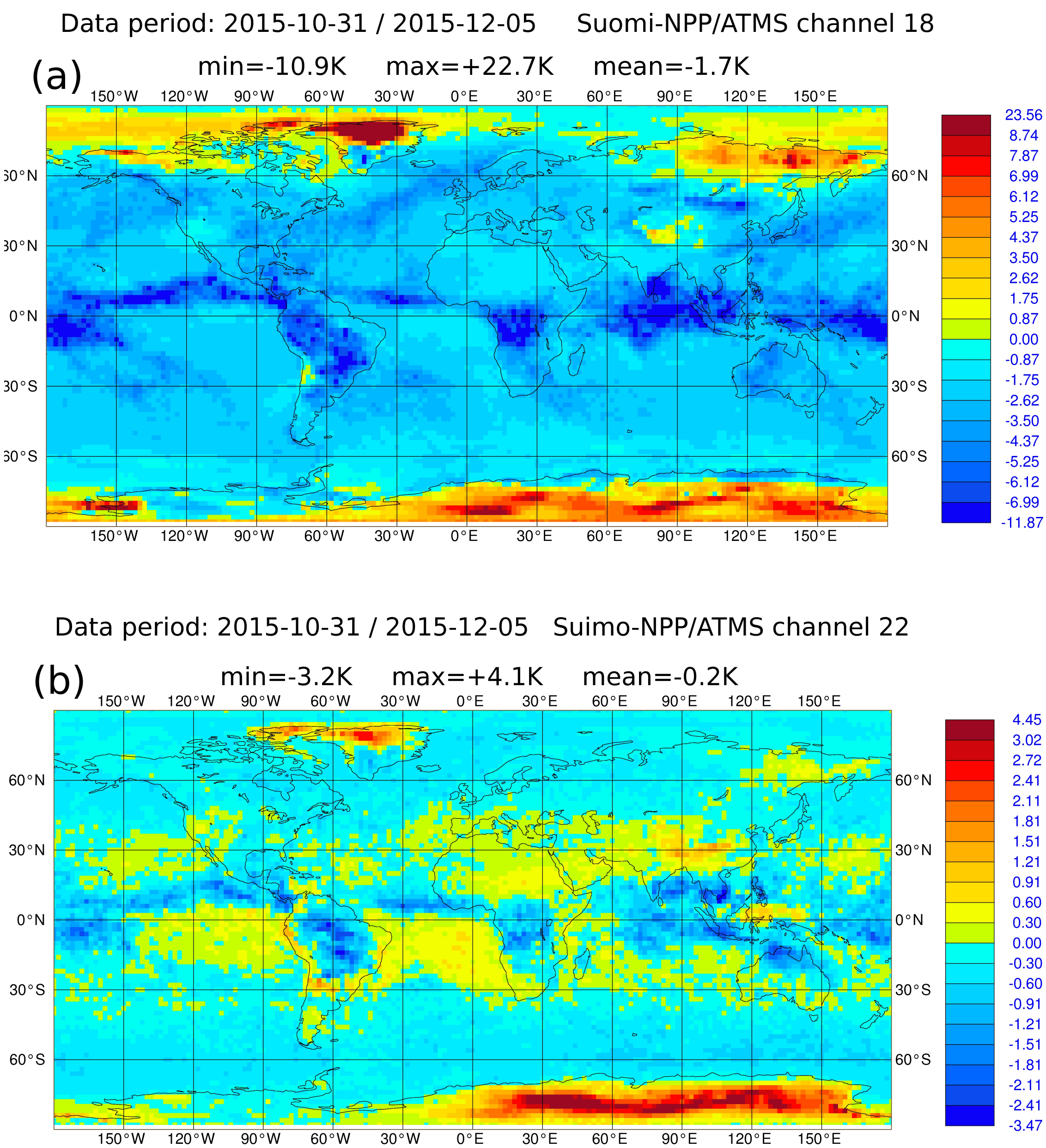

Figure 2: First-guess departures (observed BTs - those calculated from the forecast background) for Suomi-NPP/ATMS (a) channel 18 (183±7GHz) and (b) channel 22 (183±1GHz) and the current ECMWF NWP system. The maps show the mean, with the global minima, maxima and means in the captions.

Atmos. Meas. Tech. Discuss., doi:10.5194/amt-2016-9, 2016
Manuscript under review for journal Atmos. Meas. Tech.
Published: 29 January 2016

Atmospheric Measurement Techniques Discussions

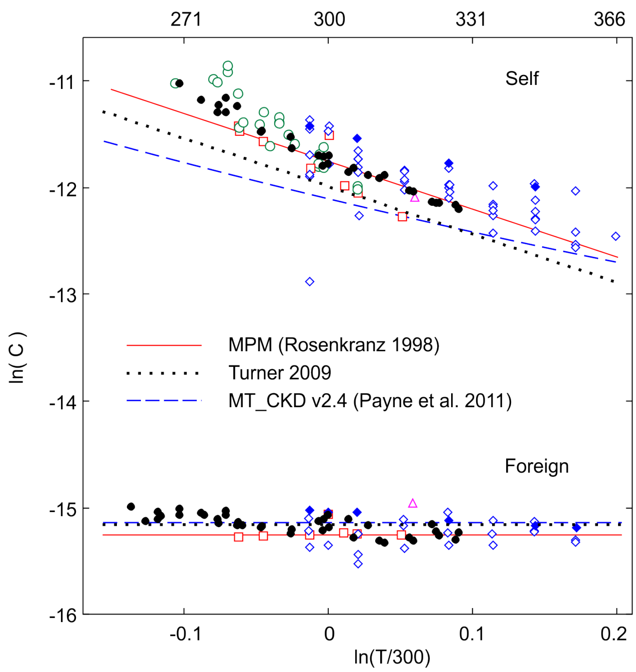

Figure 3: Self-broadened (pure water vapor or quadratic with humidity) and foreign-broadened (mixture with air or linear with humidity) continuum coefficients C (in (dB/km)/(GHz kPa)^2), as in Rosenkranz (1998, 1999). Symbols are field and laboratory data [Bauer et al., 1993 & 1995; Kuhn et al., 2002; Godon et al., 1992; Katkov et al., 1995; Liebe et al. 1984 & 1987; Koshelev et al., 2011]. Statistical uncertainty of points in each series approximately equal or less than size of points. Solid lines are continuum coefficients derived by Rosenkranz (1998) for Millimeter-wave Propagation Model (MPM). Dotted and dashed blue lines correspond to scaling of these coefficients on the basis of radiometric data suggested by Turner (2009) and Payne et al. (2011).